Electronic Supplementary Information†

Zn(II)-metal ion directed self-healing Wide Bandgap Semiconducting Supramolecular metallohydrogel: Effective non-volatile memory design for in-memory computing†

Arpita Roy,[a,ψ] Subhendu Dhibar,*[b,ψ] Kripasindhu Karmakar,[b] Sangita Some,[b] Sk Abdul Hafiz,[c] Subham Bhattacharjee,[c] Bidyut Saha*[b] and Soumya Jyoti Ray,*[a]

[a]Department of Physics, Indian Institute of Technology Patna, Bihar-801106, India.

[b]Colloid Chemistry Laboratory, Department of Chemistry, The University of Burdwan, Golapbag, Burdwan-713104, West Bengal, India.

[c]Department of Chemistry, Kazi Nazrul University, Asansol-713303, West Bengal, India.

*E-mail: *sdhibar@scholar.buruniv.ac.in* (S Dhibar); *bsaha@chem.buruniv.ac.in* (B. Saha); *ray@iitp.ac.in* (S. J. Ray).

I. Gelation ability Procedure of Zn(II)-metallohydrogel (Zn@5AP) in different solvents:

The gelation ability procedure of Zinc(II) nitrate hexahydrate and 5-Amino-1-pentanol, was tested in different solvents maintaining the minimum critical gel concentration of Zn(II)-metallohydrogel from the synthetic method of Zn(II)-metallohydrogel, described in the experimental section.[a] The gel formation strategy of Zn(II)-metallohydrogel in different solvents were checked by ‘inversion of the vial’ test. The experimental result (Table S1) clearly revealed that the Zinc(II) nitrate hexahydrate and 5-Amino-1-pentanol based mechanically stable Zn(II)-metallohydrogel can exclusively form in water medium (Fig. 1).

Table S1. Gelation process of Zn(II)-metallohydrogel[a] in various solvents[b]

Entry	Solvent[b]	Phase[c]	Conc.[d]	Vol.[e]	Gelation Time	Picture
1.	 DMF	S	297	1mL	30sec	
2.	 Hexane	I	297	1mL	-	
3.	 Cyclohexane	I	297	1mL	-	
4.	 DMSO	S	297	1mL	30sec	

5.	 m-Xylene	I	297	1mL	-	
6.	 2-butanol	I	297	1mL	-	
7.	 n-Propanol	S	297	1mL	30s	
8.	 Acetone	S	297	1mL	30s	
9.	 n-Octyl alcohol	S	297	1mL	30sec	
10.	 CH_3CN	I	297	1mL	-	
11.	 $CHCl_3$	I	297	1mL	-	

12.	 DCM	I	297	1mL	-	
13.	 MeOH	S	297	1mL	30sec	

II. Characteristics of ITO/Zn@5AP/Cu based RRAM device with multiple cycles

We have measured the complete IV curves for device 2 (ITO/Zn@5AP/Cu) for consecutive cycles and observed some variability in the first few cycles (~ 20) as shown in Fig. S1 which gets stabilised later. The initial variation can arise due to ion migration. Cu ion migration is also involved in the conductive filament formation that is responsible for switching. RRAM devices often rely on the movement of oxygen vacancies within the material to achieve resistive switching. However, with repeated cycling, the distribution and concentration of oxygen vacancies can change. This redistribution can alter the resistive states and affect the hysteresis behaviour observed in the I-V curve.

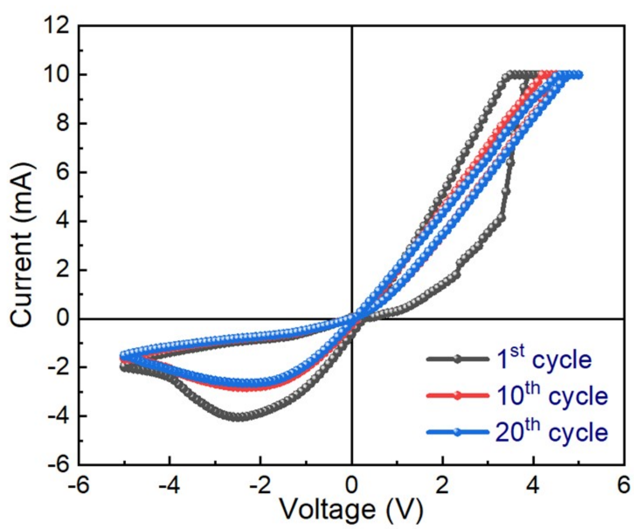

Fig. S1. I-V characteristics for glass/ITO/Zn@5AP/Cu based device device upto 20th cycle.

III. Characteristics of Cu/Zn@5AP/Cu based RRAM device with multiple cycles:

We have also measured the complete IV curves for device 3 (Cu/Zn@5AP/Cu) for consecuitive cycles and observed some variability in the first few cycles (~ 20) as shown in Fig. S2 which gets stabilised later. The initial variation can arise due to ion migration. Cu ion migration and oxygen vacancy are involved in the switching process.

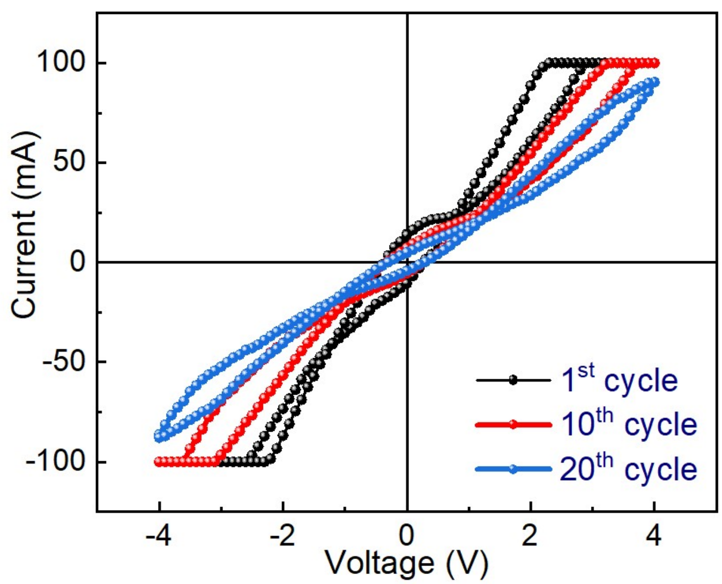

Fig. S2. I-V characteristics for glass/Cu/Zn@5AP/Cu based device upto 20th cycle

IV. Comparison of IV Characteristics in between ITO/Zn@5AP/Cu & Cu/Zn@5AP/Cu based RRAM device in one graph:

For device 2 (ITO/Zn@5AP/Cu) and device 3 (Cu/Zn@5AP/Cu), we have observed that there is a structural difference between the two devices (Fig. S3). For device 2, bottom electrode is ITO and for device 3, bottom electrode is Cu. But for both the devices, top electrode is same. We have also observed some variation in complete cyclic response. The measurements are performed on individual devices, where only one single device is present on the substrate. The primary aim of this study is to check the robustness of switching/memory performance for varied number of cycles and retention behaviour to understand the suitability of the gel material and exploring the possible device designs. In a cross-bar array, similar investigation can be scaled on a large number of identical device array of similar structure, which can be explored in details in a future study.

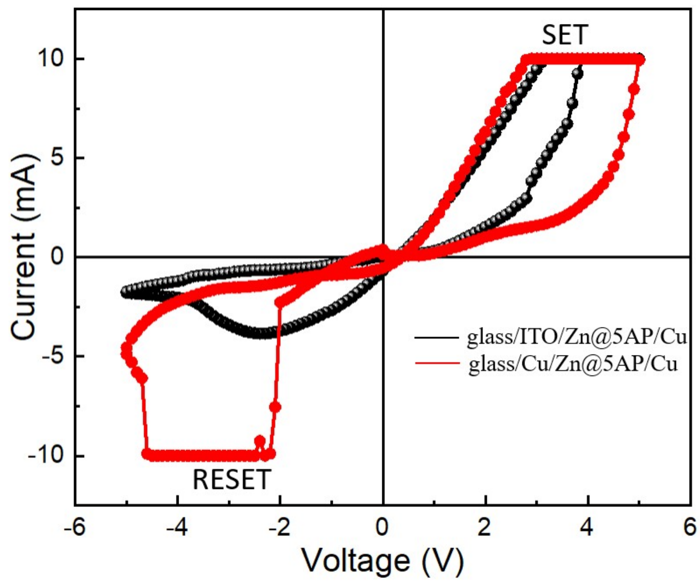

Fig. S3. I-V characteristics for device 2 and device 3

V. I-V characteristics of ITO/Zn@5AP/ITO based device at different low temperatures:

We have measured I-V characteristics of ITO/Zn@5AP/ITO based device at different low temperatures from 100K to 200K as shown in Fig. S4. From I-V characteristics we determined the conductance of this device. The conductance of this device is $2.62\times10^{-3}(\Omega\text{-m})^{-1}$. It confirms that it is showing semiconducting behavior at different low temperatures.

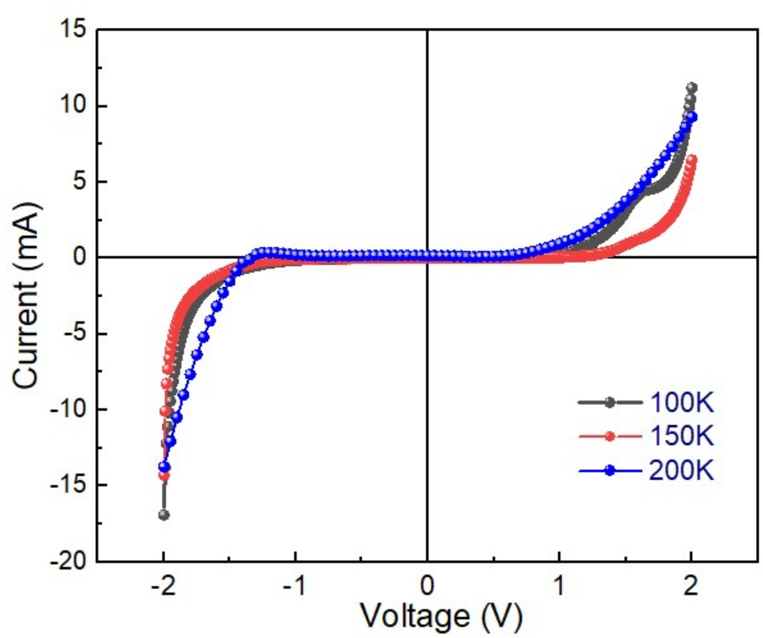

Fig. S4. I-V characteristics of ITO/Zn@5AP/ITO based device at different low temperatures from 100K to 200K.

VI. Filament formation using TEM and EDAX analysis:

We have measured IV characteristics for both devices with change in area between two electrodes. But there are no more differences in hysteresis loop for changing area between two electrodes. Therefore, we can confirm that there is formation of conduction filament which arises due to Cu ion migration. Cu ion migration plays an important role for resistive switching mechanism. We already know that under an electric field, Cu ions can travel in the direction of the applied electric field. When we apply positive voltage, Cu^{2+} ions move towards the intermediate layer, where they are reduced to metallic Cu. Then, the conductivity of this layer will increase, and Cu ions accumulate towards the bottom electrode because they will act as conductive filaments to complete the SET process and switch from HRS to LRS. The device remains in the LRS state unless a sufficient voltage with opposite parity is applied to electrochemically dissolve the Cu filament for the RESET process. When negative voltage is applied, the device enters the HRS state and the conductivity of this device decreases simultaneously. Finally, Cu^{2+} ions drift back to the top electrode. We have also observed ion migration from TEM and EDAX analysis as shown in Fig. S5(a)-(d). From TEM image, we observed the rod like structure after switching which confirms there is presence of filament during switching. From EDAX analysis, we can confirm absolutely that there is formation of Cu filament. There are 57 wt% Cu ions present in the sample after switching. In this way it provides a complete switching mechanism based on conductive filament model.

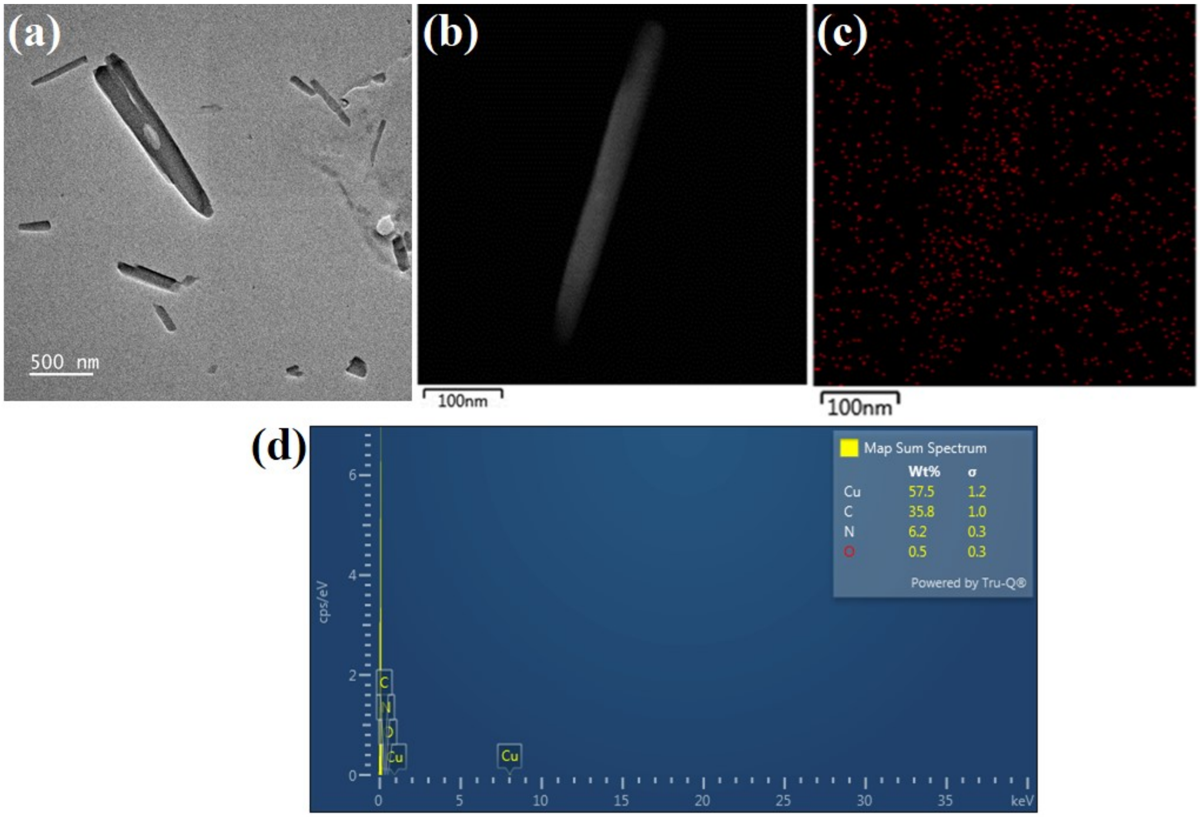

Fig. S5. (a) TEM image for the formation of Cu filament; (b-d) Elemental mapping of metallohydrogel which confirms the presence of Cu filament of 57 wt%.